Chalcogenide Letters Vol. 12, No. 10, October 2015, p. 489 - 496

INFLUENCE OF FILM THICKNESS ON OPTICAL ABSORPTION AND ENERGY GAP OF THERMALLY EVAPORATED $CdS_{0.1}Se_{0.9}$ THIN FILMS

S. A. ALY[a*], ALAA. A. AKL[a,b]
[a]*Physics Department, Faculty of Science, Minia University, Minia, Egypt*
[b]*Faculty of Science in Ad-Dawadmi, Physics Department, Shaqra University, 11911, KSA*

$CdS_{0.1}Se_{0.9}$ samples with different film thicknesses have been evaporated on ultrasonically cleaned glass substrates in a vacuum of about $8.2x10^{-4}$Pa. The film thickness was estimated using multiple-beam Fizeau fringes in reflection. The optical properties of the prepared films were studied by transmittance and reflectance measurements and the integrated absorptance (A_{UV} and A_{VIS}) in the ultraviolet and in the visible regions were calculated and correlated with film thickness. The dependence of absorption coefficient on wavelength as well as the energy gap was found to be affected by film thickness.

(Received August 16, 2015; Accepted October 5, 2015)

Keywords: Thermal evaporation, Film thickness, Integrated absorptance, Absorption coefficient, Optical energy gap.

1. Introduction

The growth of II–VI based ternary and quaternary compound semiconductors are very important due to their applications in optoelectronic devices [1], visible light emitting diodes and lasers [2], photo-electrochemical solar cells [3] and photovoltaics [4].

CdS is a very interesting material relating to photovoltaic solar cells, optoelectronics and considered as one of the most promising materials for hetero-junction thin film solar cells due to its n-type semiconductor characteristic [5,6] and wide band gap (2.44 eV).

Semiconductor compounds belonging to the Cadmium Chalcogenide family can be used for numerous technical applications like memory device, xerography, and excellent laser writer sensitivity because of their direct E_g ranging from 1.6 to 2.2 eV [7,8].

Selenium doped cadmium sulphide ($CdS_{0.1}Se_{0.9}$) thin films are very important wide band gap semiconductors (1.96 eV), because of their wide applications in optoelectronics, such as non-linear optics, visible-light emitting diodes and lasers [9, 10].

Optical energy gap is an important parameter which determines the portion of solar spectrum absorbed by photovoltaic cell. It is well known that semiconductors will absorb only photons of energy higher than the band energy gap. So, the optical band gap is the threshold for photons to be absorbed.

Ternary II–VI thin films are prepared using different deposition techniques such as, thermal evaporation [11], spray pyrolysis [12] and sputtering [13], flash evaporation [14–16], electro-deposition [17] , and chemical bath deposition [18].

Among these techniques, thermal evaporation technique is a simple method to control the deposition parameters such as substrate temperature, film thickness, evaporation rate.

*Corresponding author: saaly61@hotmail.com

Films of II–VI compounds obtained at room temperature using this method are found to be amorphous, polycrystalline, or nano-crystalline, having high resistivity and larger optical band gaps than bulk [19, 20].

The effect of film thickness on structure, optical refractive index as well as dispersion energy parameters and electrical properties of $CdS_{0.1}Se_{0.9}$ films are studied in a previous paper [11]. This work aims to study the dependence of integrated absorptance in the UV and visible regions on film thickness. Also, the absorption coefficient and optical energy gap of the prepared samples are calculated and correlated with film thickness.

2. Experimental work

2.1. Sample preparation

$CdS_{0.1}Se_{0.9}$ thin films were deposited on glass substrate by thermal evaporation technique (Edward E306A vacuum system) using high purity polycrystalline CdS powder (99.99%) and Se powder (99.999%) materials. The starting materials were subjected to grounding in an agate mortar and then prepared in pellet forms (to avoid scattering of the material). The substrates have been chemically and ultrasonically cleaned. The substrate temperature was kept constant at 523K during the deposition process. The heating source was a conventional molybdenum boat. The pressure was then brought down by the rotary pump, the oil diffusion pump was applied to the chamber until a vacuum of about $8.2x10^{-4}$ Pa was achieved.

2.2. Sample characterisation

The film thickness and deposition rate (≈ 0.5 nm/s) were in-situ controlled by a quartz crystal oscillator (Edwards model FTM3) and were correlated after deposition using multiple-beam Fizeau fringes at reflection using monochromatic light (Hg, λ_g = 546 nm)..

The structure of $CdS_{0.1}Se_{0.9}$ samples was examined in details in an earlier work [11] using a JEOL X-ray diffractometer (XRD) (Model JSDX-60PA) equipped with a Cuk_α-radiation (λ=0.145184nm). Continuous scanning was applied with a slow scanning speed (1^o/min) and a small time constant (1sec). The results of XRD analysis showed that the $CdS_{0.1}Se_{0.9}$ sample of 245 nm is in the amorphous form, while for thicker samples of 318 and 376 nm, a single phase of $CdS_{0.1}Se_{0.9}$ is formed with a hexagonal crystal structure and a preferential growth along <002> direction.

2.3. Optical measurements

The transmittance and reflectance spectra of the prepared samples were carried out at room temperature using a Shimadzu UV310PC; UV-VIS-NIR double beam spectrophotometer with a reflection attachment of V-N type (incident angle 5^o).

The integrated ultraviolet, T_{UV}, R_{UV} and visible, T_{VIS}, R_{VIS} transmittance are calculated using the following equations [21, 22],

$$\left.\begin{aligned} T_x &= \frac{\int_{\lambda_2}^{\lambda_1} T(\lambda)G(\lambda)d\lambda}{\int_{\lambda_2}^{\lambda_1} G(\lambda)d\lambda} \\ R_x &= \frac{\int_{\lambda_2}^{\lambda_1} R(\lambda)G(\lambda)d\lambda}{\int_{\lambda_2}^{\lambda_1} G(\lambda)d\lambda} \end{aligned}\right\} \quad (1)$$

where x represents UV or VIS and λ_1 and λ_2 are the integration limits, 300-380, 380-780 nm, respectively, $T(\lambda)$ and $R(\lambda)$ are the spectral transmittance and reflectance and $G(\lambda)$ is the solar spectrum at air masse (AM2).

The integrated absorptance is calculated from the following equation

$$A_x = 1 - R_x - T_x \quad (2)$$

The absorption coefficient (α) is calculated from the following relation [23, 24]

$$\alpha = \frac{1}{t} ln\left(\frac{(1-R(\lambda))}{T(\lambda)}\right) \tag{3}$$

where *t* is the film thickness (cm).

3. Results and discussion

3.1. Measurement of spectral transmittance and reflectance:

The optical properties of the investigated $CdS_{0.1}Se_{0.9}$ films were studied by spectral transmittance and reflectance. The optical measurements of transmittance T(λ) and reflectance R(λ) for $CdS_{0.1}Se_{0.9}$ samples of different film thicknesses are shown in Fig. 1 and Fig. 2, respectively. The measurements have been taken in the wavelength range 300-800 nm. An increase in the transmittance value is obtained with increasing wavelength. However, a small variation in the spectral reflectance is noticed with increasing wavelength. A decrease in both of transmittance and reflectance values was observed as the film thickness increases.

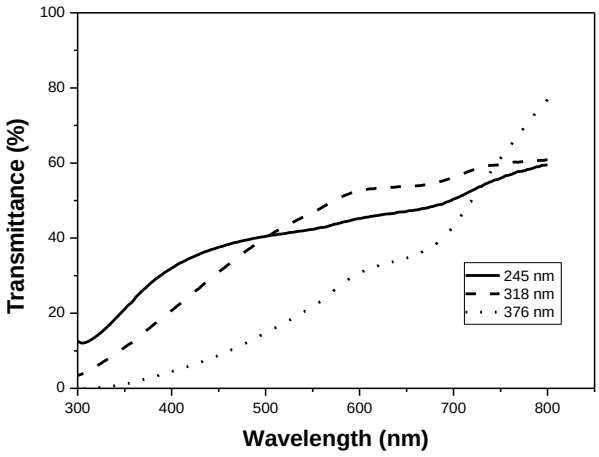

Fig.1. Spectral tranmittance vs wavelength for $CdS_{0.1}Se_{0.9}$ samples with different film thicknesses

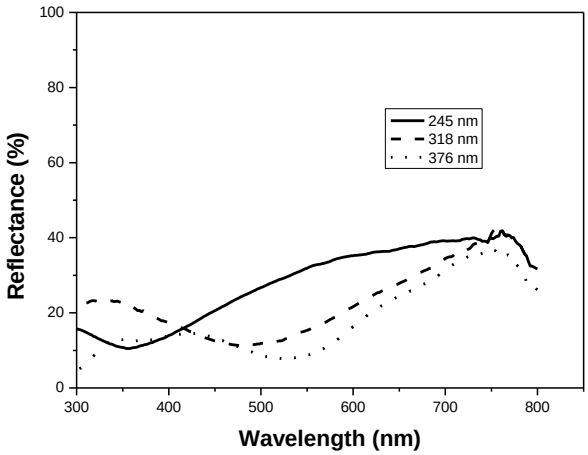

Fig.2. Spectral reflectance vs wavelength for $CdS_{0.1}Se_{0.9}$ samples with different film thicknesses

3.2. Integrated absorptance

The dependence of A_{UV} and A_{VIS} on film thickness is shown in Fig. 3 and Fig. 4. It can be noticed that the increase in film thickness enhances the absorption of light in both of UV and visible range. An increase in the values of A_{UV} from 0.68 to 0.89 with increasing thickness is obtained. Moreover, An increase in A_{VIS} with increasing thickness is observed, e.g., sample of 245 nm thickness has a value of A_{VIS} = 0.27 while that of 376 nm thickness has A_{VIS} value of 0.61, but even these values are quite low when compared with that obtained in the UV-range. So, $CdS_{0.1}Se_{0.9}$ samples of high film thicknesses can be used as an absorbing material for the UV-radiation.

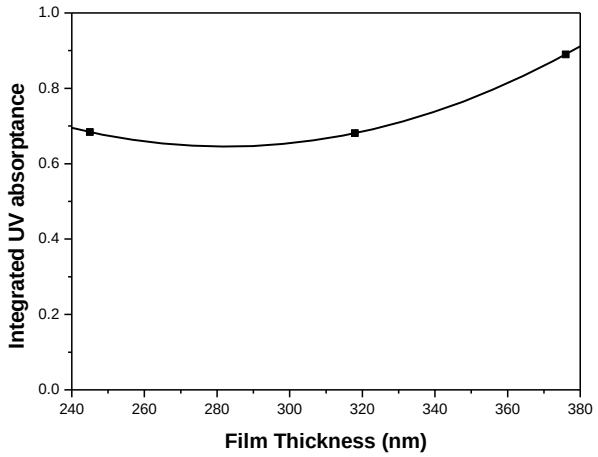

Fig.3. Integrated UV absorptance (A_{UV}) as a function of film thickness

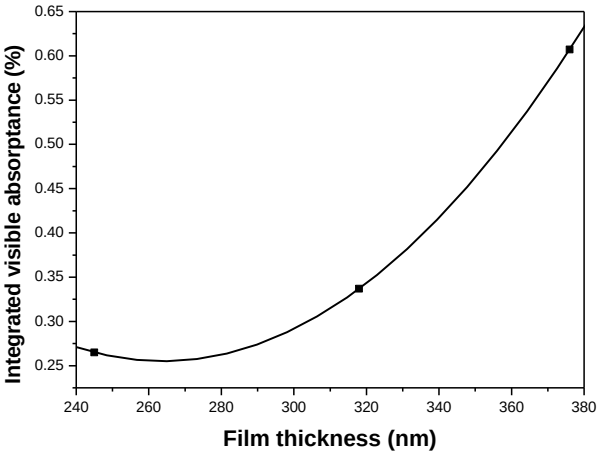

Fig.4: Integrated visible absorptance (A_{VIS}) as a function of film thickness

For thin film solar cells, absorption of light is proportional to film thickness. In order to get a complete absorption in semiconductors, the thickness of the samples should be around a few micrometers, which is unrealistic because of high and defect-related carrier recombination [25]. Many light-trapping techniques have been investigated to improve the absorption, among which a typical example is the use of scattering surface textures [26, 27]. They are balanced by the induced surface roughness that is almost of the same order as the film thickness and by the resulting large surface area which causes an increased surface recombination [25].

3.3. The absorption coefficient

The absorption coefficient has been calculated using Eq.(3) and its dependence on wavelength has been investigated at different film thicknesses and is shown in Fig. 5. For wavelengths ≥ 700 nm, no appreciable change was observed and the value of the absorption coefficient is quite low for the three samples. However, for $\lambda < 700$ nm, α is strongly dependent on wavelength. The increase in the absorption coefficient in this range is a result of transition across the semiconductor band gap in the $CdS_{0.1}Se_{0.9}$.

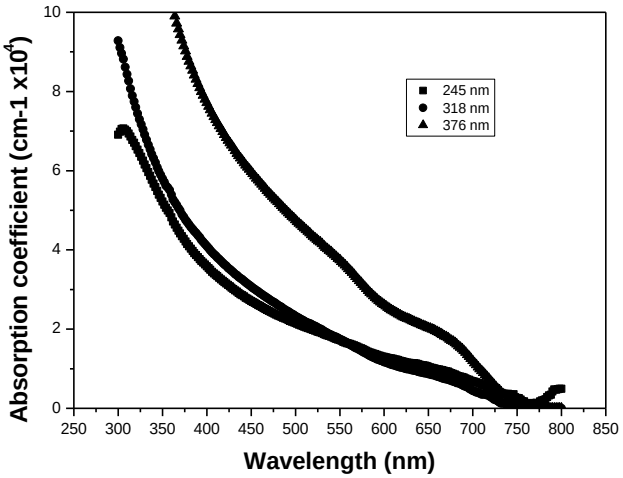

Fig.5: Absorption coefficient as a function of wavelength for $CdS_{0.1}Se_{0.9}$ Samples with different film thicknesses

3.4. Determination of Energy gap

The optical energy gap (E_g) of the films has been estimated from the following classical relation

$$\alpha = \frac{A(h\nu - E_g)^{1/2}}{h\nu}$$

where A is a constant.

The plot of $(\alpha h\nu)^2$ versus the photon energy ($h\nu$) in the absorption region indicates a direct allowed transition and is illustrated in Fig. 6 (a, b, c) for three $CdS_{0.1}Se_{0.9}$ samples of different film thicknesses. The energy gap can be determined from the extrapolation of the linear portion with the photon energy axis and its dependence on film thickness is shown in Fig.7. It can be noticed that the energy gap value is affected by film thickness. A decrease in E_g value from 2.1 (amorphous sample) to 1.95 eV (crystalline sample) as the film thickness increases from 245 nm to 376 nm, which is closed to that obtained by Yadav et al. (1.91 eV) [28].

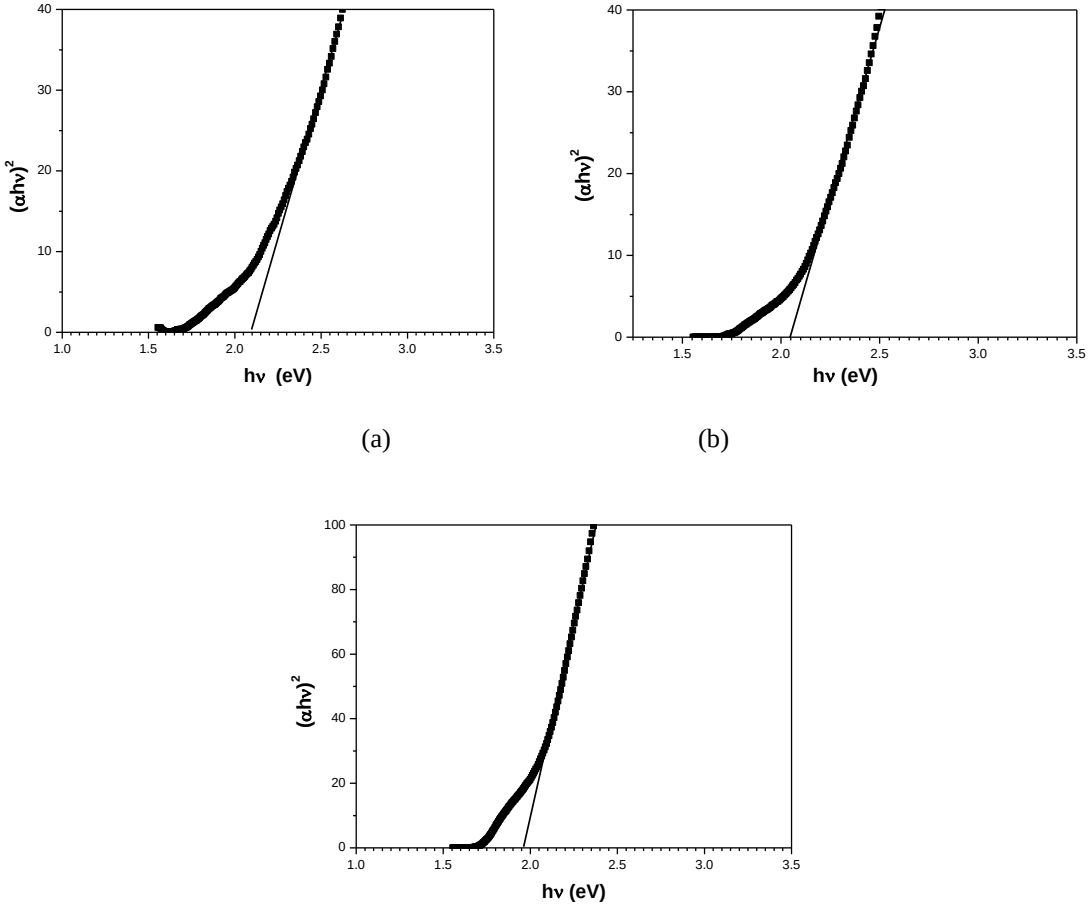

Fig.6: $(\alpha h\nu)^2$ as a function of the photon energy ($h\nu$) for $CdS_{0.1}Se_{0.9}$ samples with film thicknesses of a)245 nm, b) 318 nm and c) 376nm

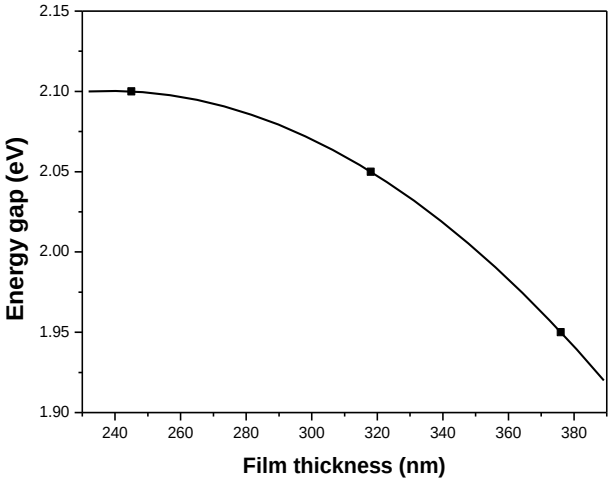

Fig.7: The energy gap value as a function of film thickness

In general, the energy gap is constant for bulk materials. However, for thin films, it is varies with thickness due to the changes in barrier height at grain boundaries with increasing film thickness. This is due to the increase in localized density of states near the band edges and in turn decreases the value of E_g with thickness. Also, the

decrease of direct band gap with the increase of film thickness can be attributed to the increase of particle size, decrease of strain and increase of lattice constant [29].

It has been proposed that charge accumulation at grain boundaries influences energy barrier associated with grain boundaries and affect barrier height [30]. The increase in barrier height is given by the following equation

$$E = E_0 + C(W - fD)^2$$

where,

E is original band width, W is barrier width, D is grain size (nm), c and f are constants depend on the carrier concentration and the accumulated charge on $_0$ grain boundaries.

It is well known that the average grain size of thin films is proportional to film thickness. So, it was expected that the band gap of will increase if charges are accumulated at grain boundaries. So, the decrease in band gap with increasing thickness infers that there is no charge accumulated at grain boundaries in the investigated films.

4. Conclusions

$CdS_{0.1}Se_{0.9}$ thin films were deposited on heated glass substrate (523 K) by thermal evaporation technique using high pure polycrystalline CdS powder (99.99%) and Se powder (99.999%) materials.

The integrated absorptance, A_{UV} and A_{VIS}, in the ultraviolet and visible region was calculated and found to be affected by film thickness. Increasing film thickness enhances the absorption of light in both of the two regions. Sample of high film thickness (376 nm) possess a high UV apbsorptance (0.89) and a quit high A_{VIS} (0.61).

The absorption coefficient,α, is found to be dependent on wavelengths lower than 700 nm as a result of transition across the semiconductor band gap in $CdS_{0.1}Se_{0.9}$. A decrease in the energy gap value from 2.1 to 1.95 eV as the film thickness increases from 245 nm to 376 nm.

References

[1] A.A. Yadav, E.U. Masumdar, J. Alloys Compd. **505**, 787 (2010).
[2] D.O. Dumcenco, Y.M. Chen, Y.S. Huang, F. Firszt, S. Łęgowski, H. Męczyńska, A. Marasek, K.K. Tiong, J. Alloys Compd. **491**, 472 (2010).
[3] A.A. Yadav, E.U. Masumdar, Sol. Energy **84**, 1445 (2010).
[4] P.A. Chate, P.P. Hankare, D.J. Sathe, J. Alloys Compd. **505**, 140 (2010).
[5] V.R. Shinde, S.B. Mahadik, T.P. Gujar, C.D. Lokhande, Appl. Surf. Sci. **252**, 7487 (2006).
[6] S. Kosea, F. Ataya, V. Bilgin b, I. Akyuza, E. Ketencic, Applied Surface Science **256,** 4299 (2010).
[7] R. Bhargava, Properties of wide band gap II-VI semiconductors. (1997) (INSEOSEC) publications, London.
[8] C. Baban, G.I. Rusu and P. Prepelita, Journal of Opto Electronics and Advanced Materials **7**(2), 817 (2005).
[9] A. Pan, H. Yang, R. Yu, B. Zou, Nanotechnology **17**, 1083 (2006).
[10] A.A. Yadav, M.A. Barote, E.U. Masumdar, Sol. Energy **84**, 763 (2010).
[11] A. A. Akl, Int, J. of Mater., Eng. and tech.nology **8**(2), 105 (2012).
[12] J.B. Chaudhari, N.G. Deshpande, Y.G. Gudage, A. Ghosh, V.B. Huse, R. Sharma, Appl. Surf. Sci. **254**, 6810 (2008).
[13] G.S. Shahane, B.M. More, C.B. Rotti, L.P. Deshmukh, Mater. Chem. Phys. **47** (1997) 263.

[14] H.J. Yu, T.H. Weng, Solid State Electron. **13**, 93 (1970)
[15] H. Weng Tung, Proc. IEEE **59**, 1503 (1971)
[16] H. Weng Tung, J. Electrochem. Soc. **126**, 1820 (1979)
[17] A.S. Baranski, W.R. Fawcett, K. Gatner, A.C. McDonald, J.R. McDonald, S. Matselen, J. Electrochem. Soc. **130**, 579 (1983)
[18] R.C. Kainthla, D.K. Pandya, K.L. Chopra, J. Electrochem. Soc. **129**, 99 (1982)
[19] S.P. Mondal, A. Dhar, S.K. Ray, Mater. Sci. Semi. Proc. **10**, 185 (2007).
[20] R.S. Singh, V.K. Rangari, S. Sanagapalli, V. Jayaraman, S. Mahendra, V.P. Singh, Sol. Energy Mater. Sol. Cells **82**, 315 (2004).
[21] C.G. Granqvist, C.M. Lampert, Science and Technology of Electrochromics, Optical Materials Technology for Energy Efficiency and Solar Energy, Toulouse, France, May 1992.
[22]S. A. Aly, Defect and Diffusion Forum, **316-317**, 23 (2011) .
[23] F. Demichelis, G. Kaniadakis, A. Tagliferro, E. Tresso, Journal of Applied Optics, **26**, 737 (1987)
[24] L. Berggren, Optical absorption and Electrical conductivity in Lithium Intercalated Amorphous Tungsten Oxide Films, Act Universitatis Upsaliensis, Uppsala, 2004.
[25] A. V .Shah, H. Schade, M. Vanecek, J, Meier, E. Vallat-Sauvain, N. Wyrsch, U, Kroll, C. Droz, J. Bailat, Prog. Photovolt: Res. Appl**. 12**, 113 (2004).
[26] W. Wang, S. Wu, K. Reinhardt, Y. Lu and S. Chen, Nano Lett., **10**(6), 2012 (2010).
[27] M. A. GreenProg. Photovolt. **10**, 2351 (2002).
[28]A.A. Yadav, E.U. Masumdar, Materials Research Bulletin, **45**, 145 (2010).
[29] S. Aksoy, Y. Cagalar, S. Ilican, M. Caglar , Optica Applicata, **XL**(1), 7 (2010).
[30] J.C. Slater, Phys. Rev., **103**, 1631 (1956).